

Giant ankyrin-G stabilizes somatodendritic GABAergic synapses through opposing endocytosis of GABA_A receptors

Wei Chou Tseng^a, Paul M. Jenkins^{b,c}, Masashi Tanaka^d, Richard Mooney^d, and Vann Bennett^{b,c,d,1}

^aDepartment of Pharmacology and Cancer Biology, Duke University, Durham, NC 27710; ^bHoward Hughes Medical Institute and ^cDepartment of Biochemistry, Duke University, Durham, NC 27710; and ^dDepartment of Neurobiology, Duke University, Durham, NC 27710

Edited by Richard L. Huganir, The Johns Hopkins University School of Medicine, Baltimore, MD, and approved December 12, 2014 (received for review September 18, 2014)

GABA_A-receptor-based interneuron circuitry is essential for higher order function of the human nervous system and is implicated in schizophrenia, depression, anxiety disorders, and autism. Here we demonstrate that giant ankyrin-G (480-kDa ankyrin-G) promotes stability of somatodendritic GABAergic synapses in vitro and in vivo. Moreover, giant ankyrin-G forms developmentally regulated and cell-type-specific micron-scale domains within extrasynaptic somatodendritic plasma membranes of pyramidal neurons. We further find that giant ankyrin-G promotes GABAergic synapse stability through opposing endocytosis of GABA_A receptors, and requires a newly described interaction with GABARAP, a GABA_A receptor-associated protein. We thus present a new mechanism for stabilization of GABAergic interneuron synapses and micron-scale organization of extrasynaptic membrane that provides a rationale for studies linking ankyrin-G genetic variation with psychiatric disease and abnormal neurodevelopment.

giant ankyrin-G | GABAergic synapses | extrasynaptic membrane | GABARAP | GABA_A receptor endocytosis

Interneurons that release γ -aminobutyric acid (GABA) are a major source of inhibitory signaling in vertebrate nervous systems, and play important roles in cognition, mood, and behavior (1, 2). Many of these inhibitory interneurons release GABA, which binds to ionotropic ligand-gated GABA_A receptors located at GABAergic synapses and at extrasynaptic sites, and these GABA_A receptors are sites of action for benzodiazepine and barbiturates (3). GABA_A receptors are dynamic, with continuous exchange between synaptic and extrasynaptic sites in the plane of the membrane, as well as endocytic trafficking between the cell surface and intracellular compartments (3–6). GABA_A receptor cell surface expression is believed to be required for formation of GABAergic synapses based on studies with heterogeneously-expressed GABA_A receptors (7). However, the role of GABA_A receptors in preserving GABAergic synapses has not yet been described in a native neuronal environment.

GABAergic synapses localize to both the axon initial segment (AIS) as well as somatodendritic sites of target neurons (2, 8, 9). In the cerebellum, basket and stellate interneurons project specific axon terminals to the AISs of Purkinje cells, forming GABAergic “pinneau” synapses (10). Formation of these pinneau synapses depends on a steep gradient of the cell adhesion molecule neurofascin, which is enriched at the AIS (11, 12). Both GABAergic pinneau synapses and the neurofascin gradient are missing in mice with cerebellar knockout out of the membrane adaptor ankyrin-G (11, 13). Ankyrin-G coordinates multiple proteins at AISs including voltage-gated sodium channels (VGSC), KCNQ2/3 channels, 186-kDa neurofascin, and beta-4 spectrin (14). A role of ankyrin-G in stabilizing GABAergic synapses outside of the AIS of cerebellar neurons has not been explored.

Assembly of AISs as well as their GABAergic synapses requires giant ankyrin-G, which contains a 7.8-kb alternatively spliced nervous system-specific exon found only in vertebrates (14). In addition to ANK repeats and a beta-spectrin-binding domain,

giant ankyrin-G (480-kDa ankyrin-G) contains 2,600 residues configured as an extended fibrous polypeptide (14–17). Giant ankyrin-G has been assumed to be confined to AISs and nodes of Ranvier and a general role for ankyrin-G in GABAergic synapse stability at other cellular sites has not been entertained (14, 15, 18).

Here we report that giant ankyrin-G is present in extrasynaptic microdomains on the somatodendritic surfaces of hippocampal and cortical neurons, and describe a giant ankyrin-G–based mechanism required for cell surface expression of GABA_A receptors and for maintaining somatodendritic GABAergic synapses. We find that somatodendritic giant ankyrin-G inhibits GABA_A receptor endocytosis through an interaction with the GABA_A receptor-associated protein (GABARAP). This previously unidentified role for giant ankyrin-G provides a newly resolved step in the formation of GABA_A-receptor-mediated circuitry in the cerebral cortex as well as a rationale for recent linkage of human mutations in the giant ankyrin exon with autism and severe cognitive dysfunction (19).

Results

Somatodendritic GABAergic Synapse Stabilization Requires Giant Ankyrin-G. Knockout of the giant exon (exon 37) of 480-kDa ankyrin-G (Fig. 1A) results in loss of all known features of the AIS including clustering of VGSCs, the cell adhesion molecule neurofascin, KCNQ2/3 channels, and beta-4 spectrin as well as assembly of microtubule bundles (16). In addition, GABAergic synapses at the AIS of cerebellar Purkinje neurons are completely lost, as illustrated by the absence of immunoreactivity for vGAT

Significance

GABA_A-receptor-based interneuron circuitry is essential for higher order function of the human nervous system and is implicated in schizophrenia, depression, anxiety disorders, and autism. GABAergic synapses are located on neuronal cell bodies and dendritic shafts as well as axon initial segments. This study demonstrates that giant ankyrin-G forms micron-scale domains on neuronal cell bodies and dendritic shafts, and promotes somatodendritic GABAergic synapse stability through interaction with GABARAP and inhibition of GABA_A receptor endocytosis. This previously undescribed mechanism for regulating cell surface expression of GABA_A receptors and maintaining GABAergic interneuron synapses offers a rationale for previous association of ankyrin-G genetic variation with neurodevelopmental disorders and psychiatric disease.

Author contributions: W.C.T., M.T., R.M., and V.B. designed research; W.C.T. and M.T. performed research; W.C.T. and P.M.J. contributed new reagents/analytic tools; W.C.T., P.M.J., and M.T. analyzed data; and W.C.T., R.M., and V.B. wrote the paper.

The authors declare no conflict of interest.

This article is a PNAS Direct Submission.

Freely available online through the PNAS open access option.

¹To whom correspondence should be addressed. Email: vann.bennett@dm.duke.edu.

This article contains supporting information online at www.pnas.org/lookup/suppl/doi:10.1073/pnas.1417989112/-DCSupplemental.

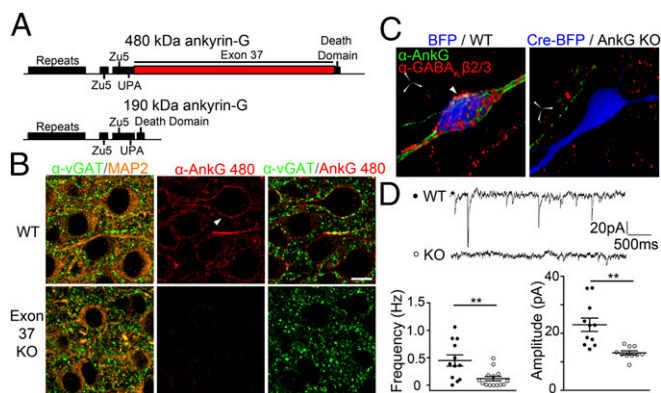


Fig. 1. Somatodendritic GABAergic synapse stability requires 480-kDa ankyrin-G. (A) Scheme of 480-kDa ankyrin-G and 190-kDa ankyrin-G. (B) Loss of somatodendritic 480-kDa ankyrin-G and GABA_A receptor in exon 37 KO pyramidal neurons. Arrowhead denotes ankyrin-G outpost on the soma. (Scale bar: 5 μ m.) (C and D) Loss of GABA_A receptor (C) and GABA_A receptor-related mIPSC frequency and amplitude (D) in cultured hippocampal ankyrin-G KO neurons. (Scale bar: 5 μ m in all axes.) ** P < 0.005 (t test, n = 10–15 per group). Error bar, SEM.

(vesicular GABA transporter), a synaptic vesicle transporter specific for presynaptic terminals of GABAergic synapses (Fig. S14) (16). These results are consistent with previous observations based on knockout of all ankyrin-G isoforms in the cerebellum (11). To determine whether loss of GABAergic synapses was limited to Purkinje neurons, we examined the hippocampal CA1 region and pyramidal neurons in the cerebral cortex in postnatal day (PND) 24 exon 37 KO mice. Surprisingly, vGAT immunolabeling was highly reduced in the cell body/AIS region in tissue sections of CA1, and also was missing from the somatic membrane as well as the AIS of individual pyramidal neurons (Fig. S1B and Fig. 1B).

To explore the role of ankyrin-G in GABAergic synapse stability in isolated neurons, we knocked out all ankyrin-G polypeptides in pyramidal neurons by transfecting cells isolated from hippocampi of exon 22–23 floxed mice (20) with a Cre-BFP plasmid. Expression of Cre-recombinase resulted in the loss of all major ankyrin-G isoforms (20), and also eliminated GABA_A receptor labeling by antibody against β 2/3 subunits at somatic as well as proximal dendrite sites in addition to the AIS (Fig. 1C). Loss of somatodendritic GABAergic synapses was not due to lack of action potential firing because GABAergic synapses were unaltered in wild-type (WT) neurons following prolonged tetrodotoxin treatment (Fig. S2).

We next determined effects of ankyrin-G knockout on GABA_A receptor function in cultured neurons using whole-cell patch clamp recordings to measure postsynaptic currents. Recordings of GABA_A receptor-dependent postsynaptic currents, isolated through pharmacological blockade of sodium channels, ionotropic glutamate receptors, and glycine receptors (V_h = -70 mV), revealed a marked reduction in the frequency and the amplitude of spontaneous miniature inhibitory postsynaptic current (mIPSC) events (Fig. 1D). This functional deficit could be rescued by expression of 480-kDa ankyrin-G-GFP (see Fig. 4E). Therefore, in addition to its established role in regulating the AIS, giant ankyrin-G also is necessary for both the structure and function of GABA_A receptor-mediated synaptic connectivity in the somatodendritic region of hippocampal neurons.

Having established the requirement of giant ankyrin-G for preserving somatodendritic GABAergic synapses, we next asked whether giant ankyrin-G itself was also present in the somatodendritic compartment. Using antibody specific for the giant exon-encoded domain, we discovered that 480-kDa ankyrin-G accumulated on both the somatodendritic plasma membrane as well as the AIS of pyramidal neurons in PND24 tissue sections of mouse brain and in DIV21 cultured hippocampal neurons (Fig. S3A and

B). In contrast, in younger tissue (PND7) and cultured neurons (DIV7), 480-kDa ankyrin-G labeling was restricted to the AIS (Fig. S3A and B). Somatodendritic plasma membrane staining for 480-kDa ankyrin-G was specific because it also was detected with a second affinity-purified antibody against the C-terminal domain of ankyrin-G, and because staining was absent in exon 37 KO mice (Fig. S3A and C). Notably, cerebellar Purkinje neurons of adult mice did not exhibit somatic ankyrin-G labeling (Fig. S14), indicating the somatodendritic localization of ankyrin-G is neuron-type specific. Interestingly, following submission of this paper, 190-kDa ankyrin-G lacking the giant exon was reported to localize to nanodomains in dendritic spines of hippocampal neurons where it contributes to NMDA receptor-dependent plasticity (21).

We next determined whether other proteins known to associate with ankyrin-G at the AIS also localize to the somatodendritic compartment of cultured hippocampal neurons. Both VGSC and neurofascin clustered on the plasma membrane of soma and proximal dendrites of cultured pyramidal WT neuron, and were absent in ankyrin-G KO neurons (Fig. S4A). In contrast, beta 4-spectrin localized exclusively to the AIS and was missing from somatodendritic sites. Beta 2-spectrin was present in the somatodendritic membrane but did not require ankyrin-G (Fig. S4B and C). Giant ankyrin-G-based somatodendritic domains thus resemble the AIS in containing VGSC and neurofascin, but differ from the AIS in that they lack beta-4 spectrin.

Having demonstrated the somatodendritic localization of 480-kDa ankyrin-G and its membrane-spanning partners, we next addressed the role of its exon 37-encoded insert in preserving GABAergic synapses. We transfected ankyrin-G KO hippocampal neurons with cDNA encoding either 190-kDa ankyrin-G (lacking exon 37) or 480-kDa ankyrin-G (containing exon 37) (Fig. 1A). Although 190-kDa ankyrin-G associated with the somatodendritic plasma membrane, only 480-kDa ankyrin-G stabilized GABAergic synapses, as marked by labeling for GABA_A receptors β 2/3 subunits (Fig. 2A), gephyrin (a postsynaptic marker of GABAergic synapses) (Fig. 2B) and vGAT (a presynaptic marker of GABAergic synapses) (Fig. 2C). Similarly, in exon 37 KO mice, GABAergic synapses were missing even though the level of 190-kDa ankyrin-G was elevated due to in-frame splicing (16). Thus, 190-kDa ankyrin-G was insufficient to support the stabilization of vGAT+ terminals in exon 37 KO neurons, even

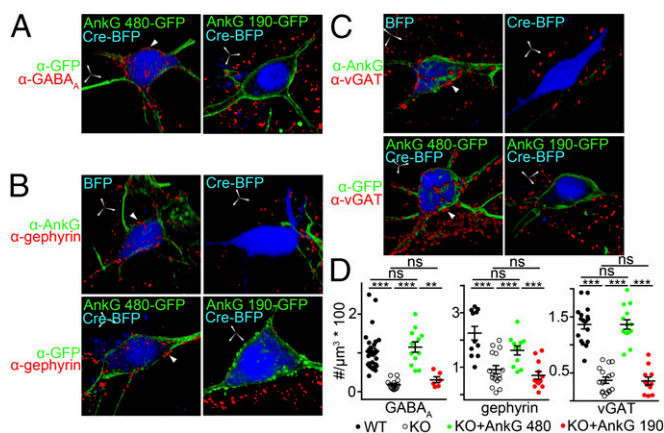


Fig. 2. The giant exon 37 of 480 ankyrin-G is required for the localization of somatodendritic GABAergic synapses in cultured neurons. (A–C) Rescue of somatodendritic GABA_A receptor (A), Gephyrin (B), and vGAT (C) in ankyrin-G KO hippocampal neurons by transfection with cDNA encoding 480-kDa ankyrin-G but not 190-kDa ankyrin-G. Arrow heads indicate GABA_A receptor, gephyrin, or vGAT clusters. (Scale bar: 5 μ m in all axes.) (D) Quantification of GABA_A receptor density in A–C. ** P < 0.005. *** P < 0.0005. ns = nonsignificant (one-way ANOVA P < 0.0001 followed by Tukey post hoc test, n = 10–15 per group). Error bar, SEM.

though it was fully capable of associating with somatodendritic membranes (Fig. 1*B* and Figs. S1 and S3*C*).

Giant Ankyrin-G Forms Micron-Scale Domains on Somatodendritic Membranes. Ankyrin-G and beta-2 spectrin colocalize in microdomains on the lateral membranes of epithelial cells that depend on palmitoylation of ankyrin-G at C70 and on binding of phosphoinositides by beta-2 spectrin (22). We therefore resolved the organization of somatodendritic ankyrin-G and its partners in cultured hippocampal neurons using deconvolution and 3D-rendering (Fig. 3). Giant ankyrin-G localized within microdomains of similar dimensions to those resolved in MDCK cells, both in sections of brain tissue as well as in cultured hippocampal neurons (Fig. 3*B*). Ankyrin-G microdomains were resolved using two different affinity-purified antibodies, which exhibited extensive colocalization (Pearson coefficient of 0.8) (Fig. 3*B*). Ankyrin-G binding partners VGSC, neurofascin, and beta-2 spectrin also colocalize in these micron-scale patches with Pearson coefficients of ~ 0.6 (Fig. 3*B* and *C*). We therefore, to our knowledge for the first time, observe developmentally regulated and cell type-specific somatodendritic microdomains containing 480-kDa ankyrin-G, VGSC, neurofascin, and beta-2 spectrin in cortical and hippocampal neurons.

We next evaluated the role of membrane-association of 480-kDa ankyrin-G using a C70A mutant of 480-kDa ankyrin-G, which cannot be palmitoylated by DHHC 5/8 (22). C70A 480-kDa ankyrin-G failed to localize to the plasma membrane and also

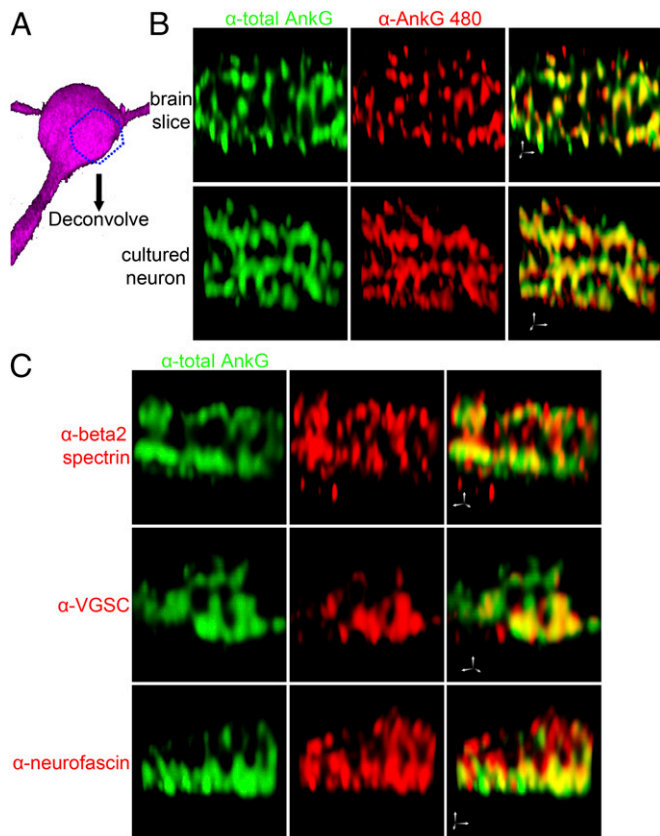


Fig. 3. Ankyrin-G micropatterns on the somatodendritic membrane together with VGSC, neurofascin, and beta-2 spectrin. (A) Schematic presentation of the cropped region on the somatodendritic membrane for imaging deconvolution in the 3D image of a neuron. (B) Antibody against 480-kDa ankyrin-G labels microdomains on the somatodendritic membrane of PND 24 cortical pyramidal neurons (Upper) and DIV 21 hippocampal neurons (Lower) highly colocalized with signals from antibody against total ankyrin-G. (Scale bar: 1 μ m in all axes.) (C) Ankyrin-G-interacting proteins VGSC, neurofascin, and beta-2 spectrin also form microdomains on the membrane organized by ankyrin-G. (Scale bar: 1 μ m in all axes.)

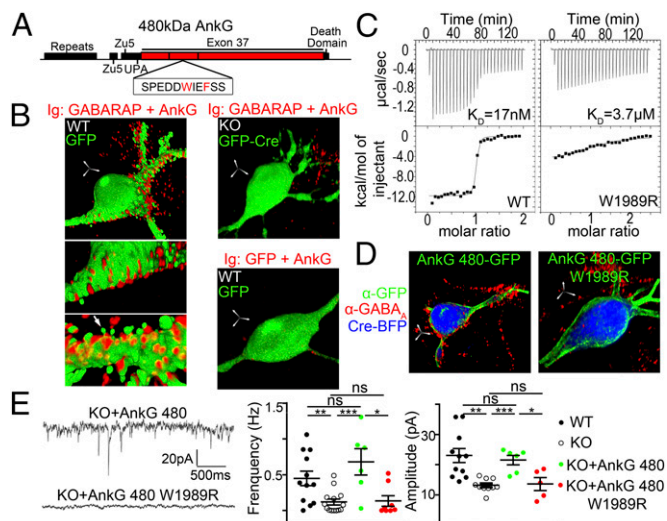


Fig. 4. Association between exon 37 of 480-kDa ankyrin-G and GABARAP is critical for GABA_A receptor clustering in hippocampal neurons. (A) Diagram of the 480-kDa ankyrin-G polypeptide and the location of LIR motif within residues 1479–2337 used in yeast two-hybrid assay. (B) Proximity ligation assay reveals in situ interaction between ankyrin-G and GABARAP that is lost in ankyrin-G KO neurons and does not occur with antibody against GFP. Arrows: spines devoid of ligation signal. (Scale bar: 5 μ m in all axes.) (C) Loss of binding of GABARAP to W1989R ankyrin-G determined by Isothermal Titration Calorimetry using GABARAP (syringe) and WT or W1989R 480-kDa ankyrin-G (residues 1819–2335) (cell). (D and E) W1989R mutation of ankyrin-G prevents rescue of GABA_A receptor clustering (D) and restoration of mIPSCs (E) in ankyrin-G KO neurons. (Scale bar: 5 μ m in all axes.) * $P < 0.05$. ** $P < 0.005$. *** $P < 0.0005$. ns, nonsignificant (One-way ANOVA $P < 0.0001$ followed by Tukey post hoc test, $n = 5$ –10 per group). Error bar, SEM.

lacked ability to restore GABAergic clusters, as illustrated by the loss of immunostaining of GABA_A receptors, gephyrin, and vGAT (Fig. S5*A*). We then examined whether specific ankyrin-G microdomains are required for stabilizing GABAergic synapses by adding the 22 amino acid, amino-terminal, myristoylation/palmitoylation motif from Lyn kinase to C70A 480-kDa ankyrin-G. Myr-Palm (MP) C70A 480-kDa ankyrin-G was restored on the somatodendritic membrane by lipid modification but was unable to rescue GABAergic synapses in ankyrin-G null neurons (Fig. S5*A* and *B*). Moreover, MP C70A 480-kDa ankyrin-G no longer formed functional microdomains on the somatodendritic membrane, as demonstrated by loss of colocalization with partner neurofascin (Fig. S5*C*). Therefore, ankyrin-G requires both its giant exon as well as its association with the plasma membrane through C70-dependent palmitoylation for the formation of giant ankyrin-G microdomains necessary for generation of GABAergic synapses.

Giant Ankyrin-G Acts Through GABARAP in Stabilizing GABAergic Synapses. We next addressed the mechanism for 480-kDa ankyrin-G-dependent stabilization of GABAergic synapses on soma and dendrites. In unbiased yeast-two hybrid screens of adult brain libraries, we identified two proteins, GABARAP and GABARAP-like 1 (GABARAPL1, or GEC1), as potential binding partners for residues 1479–2337 of the giant exon-encoded domain (Fig. 4*A* and Fig. S6). Both GABARAP and GABARAP-like 1 belong to an ubiquitin-like LC3 family, mediate intracellular trafficking and autophagy, and associate with the gamma-2 subunit of GABA_A receptors to promote their cell surface expression (23–27), features that render them well-suited to mediate giant ankyrin-G-dependent stabilization of GABAergic synapses.

We determined whether endogenous GABARAP and ankyrin-G interact in vivo using a proximity ligation assay, which identifies proteins localized within 10–15 nm of each other (28) (Fig. 4*B*). The antibody pair of goat anti-ankyrin-G (reacting with all ankyrin-G

polypeptides) and rabbit anti-GABARAP generated numerous proximity ligation puncta on the surface of somatodendritic and AIS membranes in WT neurons (Fig. 4B). In contrast, these in situ ligation signals were completely absent in ankyrin-G KO neurons. Moreover, changing the antibody pair to antibodies recognizing noninteracting molecules GFP and ankyrin-G also eliminated the ligation signal.

Having established that ankyrin-G associates with GABARAP in neurons, we next characterized the GABARAP–ankyrin-G interaction by isothermal titration calorimetry (ITC), using purified GABARAP and residues 1819–2335 of giant ankyrin-G, both expressed in bacteria. These polypeptides associated in a 1:1 stoichiometry with a $K_D \sim 20$ nM (Fig. 4C). Giant ankyrin-G and GABARAP thus associate with high affinity in vitro and are associated together in neurons on somatodendritic as well as AIS membranes.

The in situ and in vitro association of giant ankyrin-G with GABARAP/GABARAPL1 raised the possibility that this interaction contributes to preserving GABAergic synapses in vivo. We tested this hypothesis by determining synapse-forming activity of a mutant form of 480-kDa ankyrin-G that is incapable of interacting with GABARAP/GABARAPL1. GABARAP and other members of LC3 family interact with LC3-interacting (LIR) motifs (29, 30). 480-kDa ankyrin-G contains a potential LIR motif with a critical tryptophan residue (W1989) that is conserved among jawed vertebrates (Fig. 4A). We generated a W1989R mutation of giant ankyrin-G based on an uncharacterized human variant identified in the human exome sequencing project (<http://evs.gs.washington.edu/EVS/>). The W1989R mutation resulted in a 200-fold reduction in K_D of the ankyrin-G polypeptide interaction with GABARAP in ITC ($4 \mu\text{M}$ compared with 20 nM for WT) (Fig. 4C). Moreover, W1989R 480-kDa ankyrin-G failed to restore GABAergic synapses on the somatodendritic and AIS membrane, as evidenced by the lack of immunolabeling for GABA_A receptors $\beta 2/3$ subunits, gephyrin, and vGAT (Fig. 4D and Fig. S7). Furthermore, electrophysiological measurements revealed that W1989R 480-kDa ankyrin-G also was unable to restore the frequency and amplitude of GABA_A receptor-mediated mIPSCs in ankyrin-G KO cultured neurons, whereas neurons transfected with WT 480-kDa ankyrin-G displayed normal levels of GABA_A receptor-mediated synaptic activity (Fig. 4E). Importantly, W1989R 480-kDa ankyrin-G associated with the somatodendritic membrane and rescued the AIS accumulation of VGSC, neurofascin, and beta-4 spectrin (Fig. S8), indicating that it is fully functional outside of the interaction with GABARAP. Therefore, the association between GABARAP/GABARAPL1 and the giant exon-encoded domain of 480-kDa ankyrin-G is essential for stabilizing GABAergic synapses.

Giant Ankyrin-G Opposes Endocytosis of Extrasynaptic GABA_A Receptors.

The observation that ankyrin-G is required for maintaining somatodendritic GABAergic synapses raises the possibility that ankyrin-G is a structural component of these inhibitory synapses. However, giant ankyrin-G microdomains, as resolved by 3D-deconvolution (Fig. 3), are spatially distinct from regions immunolabeled for gephyrin and vGAT, which are markers for GABAergic synapses (Pearson coefficients of 0.2; Fig. 5A). Giant ankyrin-G domains did overlap with GABARAP (Pearson coefficient of 0.6), consistent with our in vitro and in situ results (Fig. 4B and C). Giant ankyrin-G also partially colocalized with GABA_A receptors (Pearson coefficient of 0.5) as detected by the antibody against $\beta 2/3$ subunits, which are present in both synaptic and extrasynaptic sites (3, 31) (Fig. 5A). In addition, ankyrin-G showed higher colocalization with GABA_A receptor $\alpha 4$ subunit, a predominantly extrasynaptic receptor component (32), compared with the synaptic GABA_A receptor $\alpha 2$ subunit (31) (Fig. S9). Taken together, these findings indicate that giant ankyrin-G is excluded from synapses and interacts with GABA_A receptors in the extrasynaptic compartment. Based on the lack of synaptic localization of ankyrin-G, it is unlikely that ankyrin-G participates directly in assembly of GABAergic synapses.

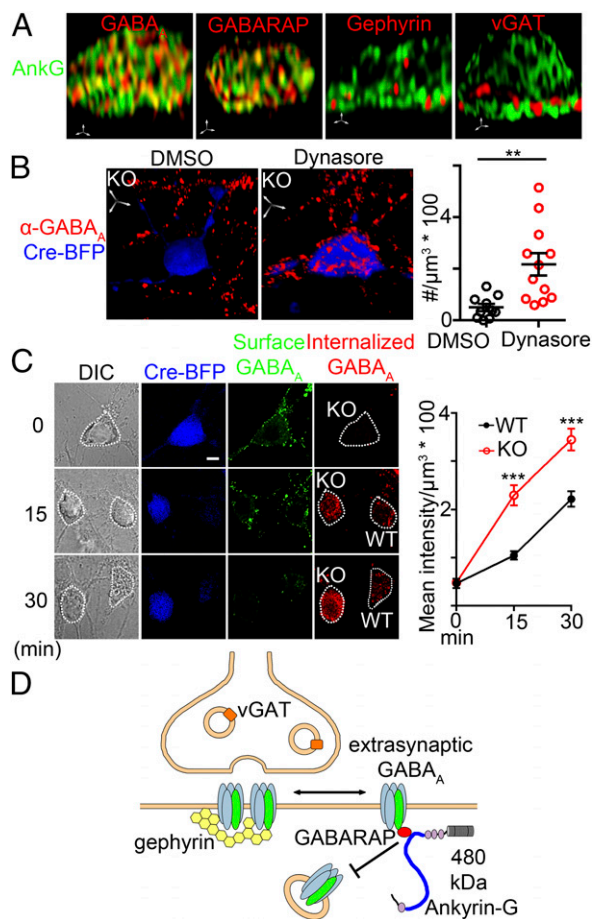


Fig. 5. 480-kDa ankyrin-G stabilizes extrasynaptic somatodendritic GABA_A receptors through inhibition of endocytosis. (A) Ankyrin-G overlaps with GABA_A receptor and GABARAP but is excluded from GABAergic synapses marked by gephyrin or vGAT in 3D-rendered high resolution images. (Scale bar: 1 μm in all axes.) (B) Dynasore (80 nM) restores GABA_A receptor in ankyrin-G KO neurons. (Scale bar: 5 μm in all axes.) $^{**}P < 0.005$ (*t* test, $n = 10$ –15 per group). Error bar, SEM. (C) GABA_A receptors undergo more rapid internalization in ankyrin-G KO neurons. See *Methods*. Dotted lines delineate individual cell. (Scale bar: 5 μm .) $^{***}P < 0.0005$ (one-way ANOVA $P < 0.0001$ followed by Tukey post hoc test, $n = 15$ –30 per group). Error bar, SEM. (D) Scheme of the role of 480-kDa ankyrin-G in localizing and stabilizing GABAergic synapses.

GABA_A receptor currents are modulated through constitutive clathrin-dependent endocytosis of GABA_A receptors from extrasynaptic sites (5, 33). Because protein levels of major GABAergic components are unchanged in exon 37 KO mice (Fig. S10A and B), we hypothesized that giant ankyrin-G stabilizes GABAergic synapses by preventing GABA_A receptor uptake from the cell surface. In support of this idea, we found that the endocytosis inhibitor dynasore (80 nM for 2 h) dramatically restored GABA_A receptor surface localization to ankyrin-G KO neurons (Fig. 5B). We directly investigated a role of ankyrin-G in opposing receptor internalization by determining rates of uptake of surface-labeled GABA_A receptors (34), and found that GABA_A receptors exhibited a significantly higher rate of intracellular accumulation in ankyrin-G KO neurons compared with WT neurons (Fig. 5C). Therefore, giant ankyrin-G prevents endocytosis of extrasynaptic GABA_A receptors through the association with GABARAP within extrasynaptic microdomains (Fig. 5D).

Discussion

Here we demonstrate that 480-kDa ankyrin-G forms developmentally regulated and cell-type specific micron-scale domains within extrasynaptic somatodendritic plasma membranes of

hippocampal and cortical neurons, and is required for stability of somatodendritic GABAergic synapses (Figs. 1–3). We further find that 480-kDa ankyrin-G acts through a newly described interaction of its giant exon-encoded sequence with GABARAP, a GABA_A receptor-associated protein (Fig. 4). Strikingly, loss of GABAergic synapses in ankyrin-G-null neurons is reversed by inhibition of endocytosis (Fig. 5). Moreover, giant ankyrin-G reduces the rate of GABA_A receptor internalization (Fig. 5). We thus present a previously undescribed mechanism, based on giant ankyrin-G, for micron-scale functional organization of the extrasynaptic membrane on the somatodendritic surface of cortical and hippocampal neurons that opposes endocytosis of GABA_A receptors and is required for stabilizing GABA_A receptor synapses.

We demonstrate the requirement for GABARAP in maintaining GABAergic innervation by showing that the W1989R mutant 480-kDa ankyrin-G, which impairs GABARAP binding, fails to rescue GABAergic clustering. GABARAP-knockdown mice showed normal GABA_A receptor targeting to the synapse and thus appeared unaffected in terms of synaptic strength (35). However, this mild phenotype likely reflects functional redundancy due to other GABARAP isoforms such as GABARAP1/GEC-1 that can also interact with both the GABA_A receptor and giant ankyrin-G. Previous work has demonstrated that GABARAP is not enriched in the gephyrin-positive postsynaptic specialization and does not anchor GABA_A receptors at the synapse (36). Consistent with this finding, we demonstrate that GABARAP colocalized with ankyrin-G at extrasynaptic sites.

Somatodendritic giant ankyrin-G microdomains, resolved here by 3D deconvolution light microscopy (Fig. 3), resemble the AIS in that they also contain VGSC and neurofascin. However, in contrast to the AIS, these somatodendritic microdomains lack beta-4 spectrin and instead have beta-2 spectrin (Fig. 3). Interestingly, giant ankyrin-G likely requires phosphorylation at S2417 to recruit beta-4 spectrin to the AIS (16). Thus, assembly of giant ankyrin-G in cell bodies and axons likely is regulated through yet to be defined but distinct sets of protein kinases and/or phosphatases. An additional level of complexity in ankyrin-G targeting is provided by the recent finding that 190-kDa ankyrin-G lacking the giant exon but otherwise capable of binding to beta spectrins and membrane protein partners localizes to nanodomains in dendritic spines (21). In addition to GABAergic synapses, somatodendritic membranes also harbor ion channels involved in regulating excitability (37). Moreover, GABARAP has multiple partners and thus likely has functions in addition to mediating GABA_A receptor localization (27, 38). Therefore, giant ankyrin-G and its GABARAP partner likely modulate cell surface behavior of yet to be discovered somatodendritic membrane proteins such as potassium and calcium channels.

A truncating mutation in the giant exon of ankyrin-G causes autism and marked cognitive dysfunction (IQ less than 50) (19). Ankyrin-G also has been linked to bipolar disorder in genome-wide association studies (39). Given that the giant exon of ankyrin-G is large and is expressed primarily in brain tissue (16), loss of function mutations are survivable but may be a source of relatively common human variation resulting in abnormal behavior, mood, and/or impaired intellectual function. An exciting possibility is that by targeting either somatodendritic giant ankyrin-G or specific components of the endocytosis machinery it may be feasible to therapeutically intervene in these inherited disorders.

Methods

Immunofluorescent Staining. The method for immunofluorescent staining was reported (40). Dissociated neurons at DIV 21 were fixed for 15 min at room temperature with 4% (wt/vol) paraformaldehyde with 4% (wt/vol) sucrose in PBS. After the PBS wash, neurons were then permeabilized for 15 min with 0.05% Triton X-100 (MP Biomedicals) in PBS and blocked with blocking buffer 5% (wt/vol) BSA in PBST. After blocking, neurons were incubated at 4 °C overnight with primary antibodies diluted in blocking buffer. On the following day, neurons were washed with PBST 3 times at 10 min each, and incubated with appropriate Alexa Fluor secondary antibodies in blocking buffer for 2 h at room temperature. Finally, cells were washed with PBST three times at 10 min each and then mounted with Prolong Gold Antifade reagent.

For VGSC staining, neurons were fixed for 15 min at room temperature with 4% (wt/vol) paraformaldehyde + 4% (wt/vol) sucrose in PBS and then permeabilized/blocked with 5% (wt/vol) fish gelatin (Sigma-Aldrich)/0.1% Triton X-100 in PBS for 30 min at room temperature. Primary antibodies were diluted in gelatin buffer and incubated with neurons for 2 h at room temperature before the secondary antibody staining as described.

The following antibody dilutions were used: rabbit anti-480-kDa ankyrin-G (1:500), goat anti-ankyrin-G (1:1,000), chicken or mouse anti-MAP2 (1:2,000), mouse anti-pan NaCh (1:100), rabbit anti-beta-4 spectrin (1:1,000), rabbit anti-beta-2 spectrin (1:500), rabbit or chicken anti-GFP (1:1,000), rabbit anti-GABARAP (1:100), rabbit anti-neurofascin (1:250), mouse anti-gephyrin (1:500), mouse anti-GABA_A receptor (1:250), guinea pig anti-VGAT (1:1,000), mouse anti-calbindin (1:1,000), and all secondary Alexa Fluor antibodies (1:250).

Electrophysiology. Whole-cell voltage-clamp recordings were made from genetically labeled hippocampal neurons at ~30 °C in oxygenated ACSF containing: 143 mM NaCl, 5 mM KCl, 5 mM Hepes, 10 mM dextrose, 1 mM MgCl₂, and 2 mM CaCl₂ (pH 7.3, adjusted with NaOH; 296 mOsm). The pipette solution contained 130 mM CsCl, 10 mM NaCl, 10 mM Hepes, 10 mM EGTA, 1 mM MgCl₂, 0.5 mM CaCl₂, 4 mM ATP-Mg, 0.4 mM GTP-Na₃, and 0.05 mM Alexa 594 hydrazide (pH 7.3, adjusted with CsOH; 295 mOsm). The pipettes were fabricated from borosilicate glass tubes and pipette resistances were 3–6 MΩ.

Data were acquired with Multiclamp 700B, low-pass filtered at 2.8 kHz, and digitized at 10 kHz. Recordings with unstable resting currents or high series resistance of > 30 MΩ were excluded from the analysis. The series resistance was compensated by 30%. After confirming that massive spontaneous excitatory postsynaptic currents could be observed in recorded hippocampal neurons, tetrodotoxin citrate (0.3 μM; Tocris), DNQX disodium salt (10 μM; Tocris), D-AP5 (25 μM; Tocris), and strychnine (1 μM; Sigma-Aldrich) were applied for ~5 min before recording GABAergic spontaneous inhibitory postsynaptic currents (IPSCs) for > 4 min at -70 mV. Recorded currents were smoothed and events that crossed the threshold of -5 pA/ms were designated as the onset of IPSCs. From these IPSCs, miniature IPSCs (mIPSCs) that had fast rise time and exponential decay were manually extracted. The frequency of mIPSCs was calculated as the number of mIPSCs divided by the recording period. The amplitude of mIPSCs was measured as the peak amplitude from the baseline, which was defined as the average of 20 ms currents just before the onset of mIPSCs. The rise time of mIPSCs was the period between 10–90% of the peak amplitude during the rise phase of mIPSCs. The decay tau was the time constant of a single exponential function that was fit to the averaged waveform of peak-normalized mIPSCs in the period between its peak and the time when it returns to the baseline-level. Neurons that generated only < 3 mIPSCs during the recording were excluded from the analysis of amplitude, rise time, and decay tau of mIPSCs. After recording mIPSCs, 1(S)-9(R)-(-)-bicuculline methiodide (10 μM; Sigma-Aldrich) was incubated in a subset of recordings, which almost completely abolished mIPSCs, indicating that the recorded mIPSCs were mediated exclusively by GABA_A receptors.

Proximity Ligation Assay. The protocol for Proximity Ligation Assay can be found on Sigma-Aldrich's website for Duolink using PLA Technology with slight modifications. Neurons at DIV 21 were fixed and incubated with primary antibodies as described in the section of immunofluorescence staining. Rabbit anti-GFP or rabbit anti-GABARAP were used in combination with goat anti-ankyrin-G. On the next day neurons were washed 3× with PBST. All remaining steps were carried out in a 37 °C humidified chamber. Neurons were first incubated with a pair of PLA probes diluted 1:10/each in PBST/5% (wt/vol) BSA for 2 h, before washing 3× at 10 min each with 1× Washing Buffer-A. Ligase was diluted 1:40 into 1× Ligation buffer and added to neurons for 1 h ligation, followed by 3 × 5 min washes with 1× Washing Buffer-A. Polymerase was then applied 1:80 to neurons in 1× amplification stock for 2 h. Neurons were washed 2 × 10 min with 1× Washing Buffer-B, 1 × 2 min with 0.01× Washing Buffer-B, and 1 × 10 min with PBST. Neurons were then incubated with primary antibody chicken anti-GFP 1:1,000 at room temperature for 2 h followed by fluorescent secondary antibody (Alexa Fluor 488 donkey-anti-chicken) for 1 h at room temperature before mounting with Prolong Gold Antifade reagent.

Dynasore Treatment and Receptor Internalization Assay. Live neurons at DIV 21 were incubated with either 80 nM dynasore or DMSO (both from Sigma-Aldrich) added to original growth media at 37 °C for 2 h before the paraformaldehyde fixation as described. Before permeabilization, neurons were incubated with antibodies raised against the extracellular epitope of GABA_A receptor β2/3 subunits (α-GABA_AR β2/3) in 5% (wt/vol) BSA/PBS at 4 °C

overnight. On the following day, neurons were washed 3 times with PBS for 10 min each before incubation with secondary antibody Alexa Fluor 488 donkey-anti-mouse (Life Technologies) for 1 h at room temperature. Finally neurons were washed with PBS 3 times at 10 min each and mounted with ProLong Gold antifade reagent (Life Technologies).

The methods for receptor internalization assay used in this study have been described (33). Live neurons were washed twice by warm Neurobasal media before incubation on ice for 1 h in the presence of high concentrations of α -GABA_AR β 2/3 (20 μ g/mL). Because receptor endocytosis was inhibited at low temperature, antibody-receptor complexes stayed on the surface during the incubation. Neurons were then washed 3 times with ice-cold Neurobasal media to remove any unbound antibody, and incubated in normal growth media without antibody at 37 °C for indicated times to allow receptor internalization. Neurons were fixed at 0, 15, 30 min with 4% (wt/vol) paraformaldehyde + 4% (wt/vol) sucrose/PBS at room temperature for

15 min, followed by incubation with excess amount of the first secondary fluorescence antibody (Alexa Fluor 488 donkey-anti-mouse 20 μ g/mL) for 2 h at room temperature to saturate all surface-bound primary antibodies. Then neurons were permeabilized with 0.25% Triton X-100/PBS for 15 min and labeled with the second secondary fluorescence antibody (Alexa Fluor 568 donkey-anti-mouse 8 μ g/mL) for 1 h at room temperature before mounting with ProLong Gold antifade reagent.

ACKNOWLEDGMENTS. We thank A. West for helpful advice; C. Vasavda for the initial yeast two-hybrid screen; K. Walder for intellectual input and characterization of the GABARAP-interacting region of ankyrin-G giant insert; K. Davis for the preparation of plasmids and yeast cotransformation experiments; J. Hostettler and E. Robinson for mouse work and the preparation of tissue sections; and J. Bear, C. Eroglu, G. Pitt, and S. Soderling for sharing plasmids and reagents. This work was funded by the Howard Hughes Medical Institute.

- Hu H, Gan J, Jonas P (2014) Interneurons. Fast-spiking, parvalbumin⁺ GABAergic interneurons: From cellular design to microcircuit function. *Science* 345(6196):1255-1263.
- Klausberger T, Somogyi P (2008) Neuronal diversity and temporal dynamics: The unity of hippocampal circuit operations. *Science* 321(5885):53-57.
- Luscher B, Fuchs T, Kilpatrick CL (2011) GABAA receptor trafficking-mediated plasticity of inhibitory synapses. *Neuron* 70(3):385-409.
- Bogdanov Y, et al. (2006) Synaptic GABAA receptors are directly recruited from their extrasynaptic counterparts. *EMBO J* 25(18):4381-4389.
- Kittler JT, et al. (2000) Constitutive endocytosis of GABAA receptors by an association with the adaptin AP2 complex modulates inhibitory synaptic currents in hippocampal neurons. *J Neurosci* 20(21):7972-7977.
- Thomas P, Mortensen M, Hosie AM, Smart TG (2005) Dynamic mobility of functional GABAA receptors at inhibitory synapses. *Nat Neurosci* 8(7):889-897.
- Fuchs C, et al. (2013) GABA(A) receptors can initiate the formation of functional inhibitory GABAergic synapses. *Eur J Neurosci* 38(8):3146-3158.
- Kole MH, Stuart GJ (2012) Signal processing in the axon initial segment. *Neuron* 73(2):235-247.
- Muir J, Kittler JT (2014) Plasticity of GABAA receptor diffusion dynamics at the axon initial segment. *Front Cell Neurosci* 8:151.
- Blot A, Barbour B (2014) Ultra-rapid axon-axon ephaptic inhibition of cerebellar Purkinje cells by the pinceau. *Nat Neurosci* 17(2):289-295.
- Ango F, et al. (2004) Ankyrin-based subcellular gradient of neurofascin, an immunoglobulin family protein, directs GABAergic innervation at purkinje axon initial segment. *Cell* 119(2):257-272.
- Kriebel M, et al. (2011) The cell adhesion molecule neurofascin stabilizes axo-axonic GABAergic terminals at the axon initial segment. *J Biol Chem* 286(27):24385-24393.
- Zhou D, et al. (1998) AnkyrinG is required for clustering of voltage-gated Na channels at axon initial segments and for normal action potential firing. *J Cell Biol* 143(5):1295-1304.
- Bennett V, Lorenzo DN (2013) Spectrin- and ankyrin-based membrane domains and the evolution of vertebrates. *Curr Top Membr* 72:1-37.
- Kordeli E, Lambert S, Bennett V (1995) AnkyrinG. A new ankyrin gene with neural-specific isoforms localized at the axonal initial segment and node of Ranvier. *J Biol Chem* 270(5):2352-2359.
- Jenkins PM, et al. (2014) Giant ankyrin-G was a critical innovation in vertebrate evolution of fast and integrated neuronal signaling. *Proc Natl Acad Sci USA* 112:957-964.
- Jones SL, Korobova F, Svitkina T (2014) Axon initial segment cytoskeleton comprises a multiprotein submembranous coat containing sparse actin filaments. *J Cell Biol* 205(1):67-81.
- Yoshimura T, Rasband MN (2014) Axon initial segments: Diverse and dynamic neuronal compartments. *Curr Opin Neurobiol* 27:96-102.
- Iqbal Z, et al. (2013) Homozygous and heterozygous disruptions of ANK3: At the crossroads of neurodevelopmental and psychiatric disorders. *Hum Mol Genet* 22(10):1960-1970.
- Jenkins PM, et al. (2013) E-cadherin polarity is determined by a multifunction motif mediating lateral membrane retention through ankyrin-G and apical-lateral transcytosis through clathrin. *J Biol Chem* 288(20):14018-14031.
- Smith KR, et al. (2014) Psychiatric Risk Factor ANK3/Ankyrin-G Nanodomains Regulate the Structure and Function of Glutamatergic Synapses. *Neuron* 84(2):399-415.
- He M, Abdi KM, Bennett V (2014) Ankyrin-G palmitoylation and β III-spectrin binding to phosphoinositide lipids drive lateral membrane assembly. *J Cell Biol* 206(2):273-288.
- Leil TA, Chen ZW, Chang CS, Olsen RW (2004) GABAA receptor-associated protein traffics GABAA receptors to the plasma membrane in neurons. *J Neurosci* 24(50):11429-11438.
- Wang H, Bedford FK, Brandon NJ, Moss SJ, Olsen RW (1999) GABA(A)-receptor-associated protein links GABA(A) receptors and the cytoskeleton. *Nature* 397(6714):69-72.
- Chen L, Wang H, Vicini S, Olsen RW (2000) The gamma-aminobutyric acid type A (GABAA) receptor-associated protein (GABARAP) promotes GABAA receptor clustering and modulates the channel kinetics. *Proc Natl Acad Sci USA* 97(21):11557-11562.
- Mansuy V, et al. (2004) GEC1, a protein related to GABARAP, interacts with tubulin and GABA(A) receptor. *Biochem Biophys Res Commun* 325(2):639-648.
- Chen ZW, Olsen RW (2007) GABAA receptor associated proteins: A key factor regulating GABAA receptor function. *J Neurochem* 100(2):279-294.
- Söderberg O, et al. (2006) Direct observation of individual endogenous protein complexes in situ by proximity ligation. *Nat Methods* 3(12):995-1000.
- Alemu EA, et al. (2012) ATG8 family proteins act as scaffolds for assembly of the ULK complex: Sequence requirements for LC3-interacting region (LIR) motifs. *J Biol Chem* 287(47):39275-39290.
- Birgisdottir AB, Lamark T, Johansen T (2013) The LIR motif - crucial for selective autophagy. *J Cell Sci* 126(Pt 15):3237-3247.
- Nusser Z, Sieghart W, Somogyi P (1998) Segregation of different GABAA receptors to synaptic and extrasynaptic membranes of cerebellar granule cells. *J Neurosci* 18(5):1693-1703.
- Chandra D, et al. (2006) GABAA receptor alpha 4 subunits mediate extrasynaptic inhibition in thalamus and dentate gyrus and the action of gaboxadol. *Proc Natl Acad Sci USA* 103(41):15230-15235.
- Kittler JT, et al. (2005) Phospho-dependent binding of the clathrin AP2 adaptor complex to GABAA receptors regulates the efficacy of inhibitory synaptic transmission. *Proc Natl Acad Sci USA* 102(41):14871-14876.
- Goodkin HP, Yeh JL, Kapur J (2005) Status epilepticus increases the intracellular accumulation of GABAA receptors. *J Neurosci* 25(23):5511-5520.
- O'Sullivan GA, Kneussel M, Elazar Z, Betz H (2005) GABARAP is not essential for GABA receptor targeting to the synapse. *Eur J Neurosci* 22(10):2644-2648.
- Kneussel M, et al. (2000) The gamma-aminobutyric acid type A receptor (GABAAR)-associated protein GABARAP interacts with gephyrin but is not involved in receptor anchoring at the synapse. *Proc Natl Acad Sci USA* 97(15):8594-8599.
- Lai HC, Jan LY (2006) The distribution and targeting of neuronal voltage-gated ion channels. *Nat Rev Neurosci* 7(7):548-562.
- Mohrlüder J, Hoffmann Y, Stangler T, Hänel K, Willbold D (2007) Identification of clathrin heavy chain as a direct interaction partner for the gamma-aminobutyric acid type A receptor associated protein. *Biochemistry* 46(50):14537-14543.
- Ferreira MA, et al.; Wellcome Trust Case Control Consortium (2008) Collaborative genome-wide association analysis supports a role for ANK3 and CACNA1C in bipolar disorder. *Nat Genet* 40(9):1056-1058.
- He M, Tseng WC, Bennett V (2013) A single divergent exon inhibits ankyrin-B association with the plasma membrane. *J Biol Chem* 288(21):14769-14779.

Supporting Information

Tseng et al. 10.1073/pnas.1417989112

SI Methods

Tissue Preparation and Immunohistochemistry. Mice at postnatal day 24 were anesthetized and killed by cardiac perfusion before removal of their brains and fixation in 4% (wt/vol) paraformaldehyde overnight. Tissue was dehydrated through a standard paraffin embedding protocol using increasing concentrations of ethanol followed by clearing in xylene and infiltration with molten paraffin in a vacuum oven. For long term storage and preservation, paraffin sections were cut at 7 μm using a Leica RM2155 rotary microtome and then mounted onto microscope slides. Embedding material was removed by Histo-Clear (VWR) and rehydrated using decreasing concentrations of ethanol followed by PBS. For antigen retrieval, samples were boiled for 20 min in 10 mM sodium citrate. Slides were then cooled, washed in PBS, blocked using blocking buffer [5% (wt/vol) fish skin gelatin in PBS containing 0.1% Triton X-100], and incubated with primary antibodies in blocking buffer. On the following day, sections were washed by PBS-0.2% Tween 20 (Calbiochem) (PBST) and incubated with secondary fluorescent antibodies in blocking buffer at room temperature for 2 h. Finally, sections were washed in PBST, mounted with Prolong Gold Antifade reagent (Life Technologies), edges sealed with nail polish, and stored at 4 $^{\circ}\text{C}$.

DNA Constructs. 190 kDa (1) and 480 kDa (2) ankyrin-G-GFP were previously described. W1989R 480-kDa ankyrin-G-GFP was generated using the Quikchange II XL mutagenesis kit (Agilent). CAG-Cre-2A-BFP plasmid was generated by cloning a Cre recombinase, a viral 2A peptide, and a TagBFP (a gift from James Bear, University of North Carolina, Chapel Hill) into pLenti6-V5-DEST viral vector (Invitrogen) with its promoter replaced by CAG (a gift from Scott Soderling, Duke University). CAG-pEGFP-N1 plasmid was acquired by replacing CMV promoter from pEGFP-N1 (Addgene) with CAG promoter. CAG-pEBFP-N1 plasmid was generated by replacing GFP with TagBFP in CAG-pEGFP-N1 vector. CAG-Cre-2A-GFP plasmid was obtained by cloning a Cre and a 2A peptide into CAG-pEGFP-N1 vector. Full-length GABARAP was pulled out from mouse brain library using yeast two-hybrid and cloned into pGEX/MAL expression vector. WT or W1989R giant insert region from residue 1819–2535 was cloned into pGEX/MAL expression vector.

Antibodies. Rabbit anti-480-kDa ankyrin-G (2), rabbit anti-beta-4 spectrin (2), goat anti-C-terminal (total) ankyrin-G (3), rabbit anti-neurofascin FNIII (4), and rabbit anti-GFP (5) antibodies were previously described. Rabbit anti-beta-2 spectrin antibody was generated using an epitope consisting of human beta-2 spectrin repeats 4–9. Chicken anti-MAP2 (ab5392) and anti-GFP (ab13970) antibodies were from Abcam. Mouse anti-pan NaCh (S8809), mouse anti-MAP2 (M4403), and mouse anti-calbindin (C9848) antibodies were from Sigma-Aldrich. Mouse anti-GABA_A receptor β 2/3 subunit (MAB341) antibody was from EMD Millipore. Guinea pig anti-VGAT (131 004) and mouse anti-gephyrin (147 021) antibodies were from Synaptic Systems. Rabbit anti-GABARAP (FL-117) antibody was from Santa Cruz. All AlexaFluor-conjugated secondary antibodies were from Life Technologies.

Neuronal Culture. Preparation of hippocampal cultures has been described (6). Hippocampi of P0 mouse pups were dissected in cold 1 \times Hank's Balanced Salt Solution (HBSS)/10 mM Hepes (Life Technologies) and incubated for 15–20 min at 37 $^{\circ}\text{C}$ with 0.25% trypsin and 100 $\mu\text{g}/\text{mL}$ DNase (Sigma-Aldrich). Hippocampi

were then washed 2 \times with Neurobasal-A plating medium (Life Technologies) containing 10% (vol/vol) FBS, 1 \times B27 supplement, 2 mM glutamine, and 1 \times Penicillin/Streptomycin (Pen/Strep) (Life Technologies). After wash, hippocampi were triturated by fire-polished glass pipettes, and filtered through 100- μm cell strainers to obtain dissociated cells in suspension. Cells were plated onto poly-D-lysine and laminin (Sigma-Aldrich) coated MatTek dishes. On the following day, neurons were first washed twice with plain Neurobasal-A and medium was replaced with growth medium containing B27, glutamin, Pen/Strep, and 1% FBS in Neurobasal-A. For tetrodotoxin experiments, 1 μM tetrodotoxin (Tocris Bioscience) was added to growth media after transfection and replenished every 5 d.

Transfection and Rescue. Calcium phosphate transfection was used to introduce DNA/ Ca^{2+} phosphate complexes directly onto the cell layer at days 3 in vitro (DIV 3) (7). Generally, 1 μg of cDNA in a 25- μL CaCl_2 /water solution was mixed with 2 \times Hank's Balanced Salt Solution followed by gentle vortexing (Clontech). The DNA- Ca^{2+} -phosphate complex was formed after incubation for 15 min at room temperature and then added dropwise to DIV 3 neurons prewashed with Neurobasal media on Mat-tek plates. Cells were incubated in a humidified 5% CO_2 chamber at 37 $^{\circ}\text{C}$ for 1 h. Precipitate was dissolved by incubating cells with Neurobasal media pre-equilibrated in 10% CO_2 in a humidified 5% CO_2 chamber at 37 $^{\circ}\text{C}$ for 20 min. Finally, cells were fed with original growth media containing 2.5 $\mu\text{g}/\text{mL}$ Ara-C and maintained until DIV 21 for immunofluorescence staining as described below.

Neurons dissociated from homozygous exon 22–23 flox/flox pups were cultured as described (6). To obtain the ankyrin-G KO background, neurons were transfected with 1 μg of CAG-Cre-2A-BFP to excise ankyrin-G in vitro or -GFP plasmid as a control. For rescue experiments, 0.5 μg of CAG-Cre-2A-BFP plus 0.5 μg of CAG-GFP rescue plasmid were used. For control experiments, 1 μg of CAG-pEBFP-N1 or CAG-pEGFP-N1 plasmid was used for cell-filling in exon 22–23 flox/flox neurons.

Protein Purification and Isothermal Titration Calorimetry. N-terminal His- and C-terminal maltose binding protein double-tagged GABARAP and WT or W1989R unstructured region of 480-kDa ankyrin-G (residues 1819–2535) were expressed in BL-21 cells subject to induction with 1 mM Isopropyl β -D-1-thiogalactopyranoside (IPTG) and frozen at -80°C overnight. On day 2, the cell pellets were solubilized and sonicated in NiNTA buffer (50 mM phosphate buffer pH 7.4, 0.3 M NaBr, 20 mM imidazole, 1 mM NaN_3 , 0.5 mM EDTA, 0.5 mM DTT, 100 $\mu\text{g}/\text{mL}$ AEBSEF, 100 $\mu\text{g}/\text{mL}$ benzamidine, 20 $\mu\text{g}/\text{mL}$ leupeptin, and 10 $\mu\text{g}/\text{mL}$ pepstatin) with 1% Triton X-100 and centrifuged at 100,000 $\times g$ at 4 $^{\circ}\text{C}$ for 1 h. The lysates were collected, incubated with NiNTA Sepharose (GE Healthcare), and rotated at 4 $^{\circ}\text{C}$ overnight. On day 3, the NiNTA resins were loaded onto columns, washed with 30 column-volume (CV) NiNTA buffer, and eluted with NiNTA buffer with 0.3 M imidazole at 2 mL per fraction. The protein-containing fractions were pooled and incubated with amylose Sepharose beads (NEB Lab) rotating at 4 $^{\circ}\text{C}$ overnight. On day 4, amylose beads were washed first with 15CV NiNTA buffer with 0.3 M imidazole and then 15 CV precision protease buffer (50 mM Tris-Cl pH 7.0, 150 mM NaCl, 1 mM EDTA, and 1 mM DTT). Beads were re-suspended in equal volume of precision protease buffer with 100 units Precision Protease (GE Healthcare) at 4 $^{\circ}\text{C}$ overnight. On day 5, eluent was collected and incubated with GST beads rotating

at 4 °C for 2 h to remove Precision Protease, and the suspension was concentrated and used directly for Isothermal Titration Calorimetry.

Isothermal Titration Calorimetry (ITC) was performed by an ITC-200 (MicroCal) at 20 °C using the protocol described here (8). The concentrations of purified GABARAP and ankyrin-G insert region were calculated by Bradford Reagent (Bio-Rad) using a UV-VIS spectrophotometer (Shimadzu Scientific) at wavelength 595 nm. Cell solutions containing 20 μM WT or W1989R insert region was titrated with 30 injections of 10 μL per each syringe solution containing 200 μM GABARAP. Experiments were repeated three times to confirm the final thermodynamic parameters and stoichiometry values. The binding curves were fitted with a single site binding model in Microcal Origina software (Originlab Corporation) to obtain the binding enthalpy (ΔH), entropy (ΔS), stoichiometry (n), and the dissociation constant (K_D).

Western Blotting. Adult mice brains were dissected on ice and homogenized in 5 volume (μL)/weight (mg) buffer (0.32 M sucrose, 10 mM phosphate buffer pH 7.4, 1 mM EDTA, 1 mM NaN₃, 100 μg/mL AEBSF, 100 μg/mL benzamidine, 20 μg/mL leupeptin, and 10 μg/mL pepstatin) using a dounce homogenizer. Lysates were mixed 1:1 with 5× PAGE buffer [25% (wt/vol) sucrose, 5% (wt/vol) SDS, 50 mM Tris pH 8, 5 mM EDTA, and bromophenol blue], sonicated for 10 pulses, and heated to 65–70 °C for 10 min. Samples (10 μL/each) were loaded on a 3.5–17.5% gradient gel in 1× Tris buffer (40 mM Tris pH 7.4, 0.2% SDS, 20 mM NaOAc, and 2 mM EDTA) until the dye front diffused out of the bottom. The gel was transferred to nitrocellulose at 300 mA overnight at 4 °C in 0.5× Tris buffer (20 mM Tris pH 7.4 and 0.01% SDS). Membranes were blocked with

blotting buffer (150 mM NaCl, 10 mM phosphate buffer pH 7.4, 0.2% Triton X-100, 1 mM NaN₃, and 1 mM EDTA) with 2% (wt/vol) BSA (Gemini Bioproducts) at room temperature for 1 h before incubation overnight at 4 °C with primary antibodies diluted in blocking buffer. On the next day, membranes were washed and incubated with I¹²⁵-labeled protein A/G 1:1,000 at room temperature for 2 h before washing and subsequent exposure on a phosphor screen. Given that protein A/G has lower affinity toward mouse IgG subclasses, membranes blotted with mouse primary antibody were incubated with a secondary rabbit anti-mouse IgG diluted 1:2,500 (Pierce) in blocking buffer before incubation with protein A/G. Radioactive signals were detected using a Typhoon imager (GE Healthcare).

Image Acquisition and Data Analysis. Samples were imaged on a Zeiss LSM 780 with a 40× 1.3 Plan-Apochromat objective and excitation was accomplished using 405-, 488-, 561-, and 633-nm lasers. Each experiment was repeated at least three independent times. Measurements were taken using Volocity (PerkinElmer) and ImageJ software. For the quantification of GABAergic synapse density, each background subtracted region of interest was drawn around the soma and proximal dendrites and converted to an 8-bit binary file. The number and the size of synaptic clusters were determined by ImageJ and normalized to the volume corresponding to each region. Conversion, threshold, and calculation parameters were kept constant for every image of each antibody staining. Statistical analysis was performed and presented using Graphpad Prism software. Data shown were mean ± SEM. Student's *t* test was used for comparisons between two groups, and a one-way ANOVA with Tukey post hoc test was used to compare three or more groups.

1. Kizhatil K, Bennett V (2004) Lateral membrane biogenesis in human bronchial epithelial cells requires 190-kDa ankyrin-G. *J Biol Chem* 279(16):16706–16714.
2. Jenkins PM, et al. (2014) Giant ankyrin-G was a critical innovation in vertebrate evolution of fast and integrated neuronal signaling. *Proc Natl Acad Sci USA*, 10.1073/pnas.1416544112.
3. He M, Abdi KM, Bennett V (2014) Ankyrin-G palmitoylation and βII-spectrin binding to phosphoinositide lipids drive lateral membrane assembly. *J Cell Biol* 206(2):273–288.
4. Davis JQ, Lambert S, Bennett V (1996) Molecular composition of the node of Ranvier: Identification of ankyrin-binding cell adhesion molecules neurofascin (mucin+/third FNIII domain-) and NrCAM at nodal axon segments. *J Cell Biol* 135(5):1355–1367.
5. Kizhatil K, Baker SA, Arshavsky VY, Bennett V (2009) Ankyrin-G promotes cyclic nucleotide-gated channel transport to rod photoreceptor sensory cilia. *Science* 323(5921):1614–1617.
6. He M, Tseng WC, Bennett V (2013) A single divergent exon inhibits ankyrin-B association with the plasma membrane. *J Biol Chem* 288(21):14769–14779.
7. Jiang M, Chen G (2006) High Ca²⁺-phosphate transfection efficiency in low-density neuronal cultures. *Nat Protoc* 1(2):695–700.
8. Wang C, Chung BC, Yan H, Lee SY, Pitt GS (2012) Crystal structure of the ternary complex of a Nav C-terminal domain, a fibroblast growth factor homologous factor, and calmodulin. *Structure* 20(7):1167–1176.

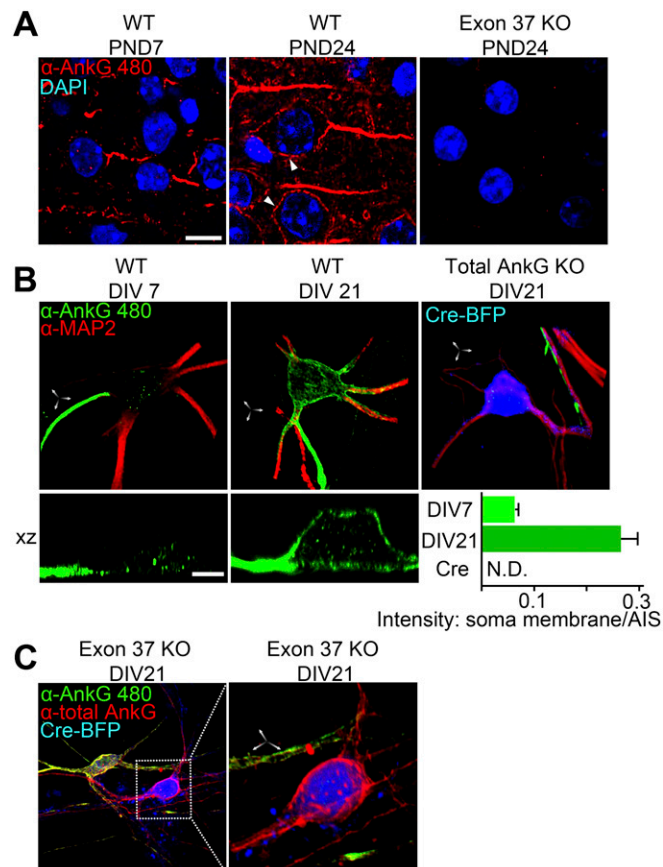


Fig. S3. Somatodendritic 480-kDa ankyrin-G is developmentally regulated in vivo and in vitro. (A) Somatodendritic accumulation of 480-kDa ankyrin-G only appears after PND 24 in WT cortical pyramidal neurons, whereas no 480-kDa ankyrin-G staining is detected in exon 37 KO brain. Arrowhead denotes ankyrin-G outpost on the soma. (Scale bar: 5 μ m.) (B) In neurons dissociated from exon 22–23 flox/flox mice, 480 ankyrin-G clusters on both the AIS and somatodendritic membrane after DIV 21 in BFP-transfected neurons but not in neurons expressing Cre. (Scale bar: 5 μ m in all axes.) x-z view shows the height of the somatodendritic membrane delineated by 480-kDa ankyrin-G staining (left). The ratio of somatodendritic membrane to the AIS at different developmental stages is quantified (right). (Scale bar: 5 μ m.) (C) The remaining staining from the antibody against total ankyrin-G in exon 37 KO neurons indicates the presence of 190-kDa ankyrin-G on the somatodendritic membrane. Dotted box shows the region of magnified soma. (Scale bar: 5 μ m in all axes.)

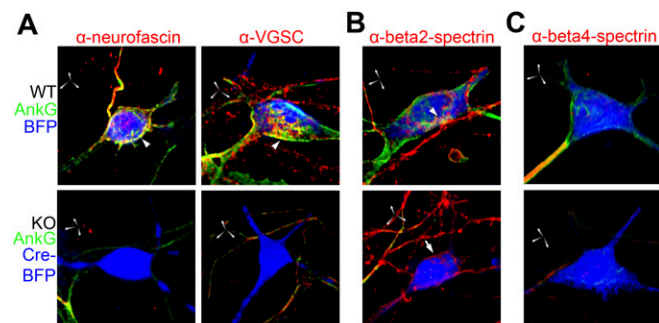


Fig. S4. Ankyrin-G is required for the somatodendritic localization of voltage-gated sodium channel and neurofascin but not spectrins. (A) Both VGSC and neurofascin accumulate on the somatodendritic membrane as well as the AIS of WT neurons but not ankyrin-G KO neurons. Arrowheads indicate neurofascin or VGSC outposts on the soma of WT neurons. (B) Beta-2 spectrin also exists on the somatodendritic membrane, whereas its accumulation persists in ankyrin-G KO neurons. Arrowhead denotes beta-2 spectrin clusters on the soma of the WT neuron, and the arrow marks the presence of beta-2 spectrin on the soma of an ankyrin-G KO neuron. (C) Beta-4 spectrin only concentrates on the AIS of the WT neuron. (Scale bar: 5 μ m in all axes.)

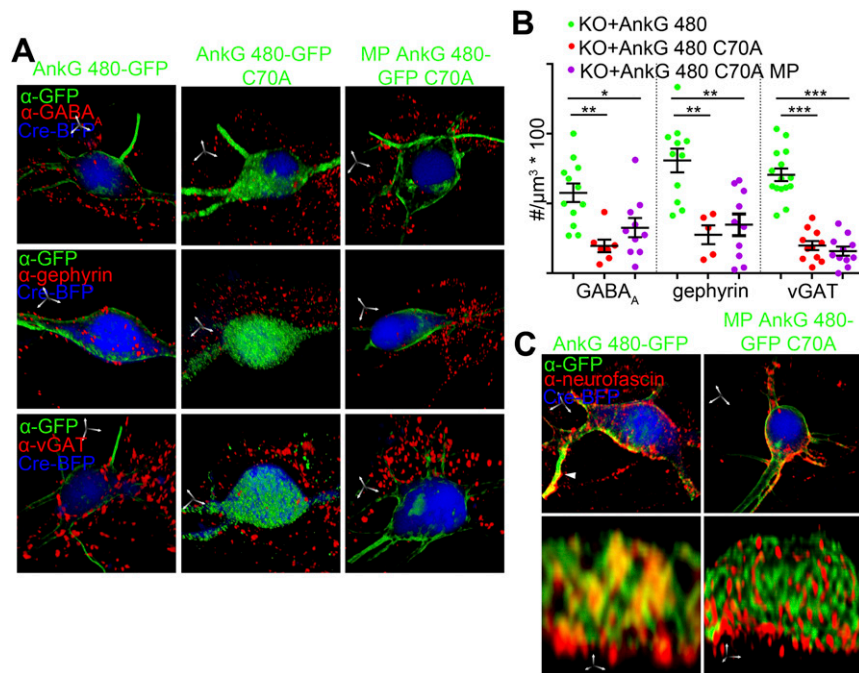


Fig. 55. Both the association of Ankyrin-G with plasma membrane and the formation of specific microdomains are required for GABAergic synapse stability. (A) C70A 480-kDa ankyrin-G and MP C70A 480-kDa ankyrin-G were both unable to rescue the clustering of GABA_A receptor, gephyrin, or vGAT. (Scale bar: 5 μm in all axes.) (B) Quantification of A. **P* < 0.05. ***P* < 0.005. ****P* < 0.0005 (unpaired *t* test, *n* = 10–15 per group). Error bar, SEM. (C) In contrast to WT 480-kDa ankyrin-G which colocalizes with neurofascin on the somatodendritic plasma membrane, MP C70A 480-kDa ankyrin-G does not form functional microdomains as suggested by the loss of neurofascin colocalization.

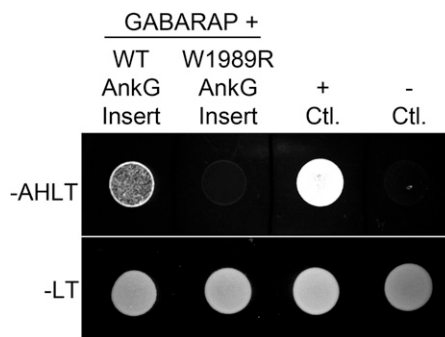


Fig. 56. Yeast two-hybrid assay identifies GABARAP as potential binding partner of insert region. A representative yeast two-hybrid assay demonstrates the binding between full length GABARAP and the residues 1479–2337 in 480-kDa ankyrin-G. The point mutation W1989R in residue 1479–2337 abolishes the interaction with GABARAP. Positive (RanBPM + pGAD) and negative control (T7 + pGAD) are shown on the right. (Upper) Minus AHLT plate. (Lower) Minus LT plate.

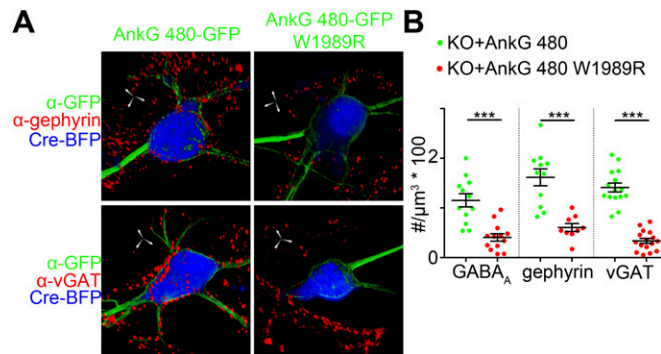


Fig. 57. W1989R 480-kDa ankyrin-G cannot rescue the GABAergic clustering on the membrane of ankyrin-G KO neurons. (A) In contrast to the restoration of GABAergic innervations with WT 480-kDa ankyrin-G, W1989R 480-kDa ankyrin-G fails to accumulate gephyrin or vGAT on the somatodendritic membrane and the AIS of ankyrin-G KO neurons. (Scale bar: 5 μm in all axes.) (B) Quantification of A including results from Fig. 3. *** $P < 0.0005$ (unpaired t test, $n = 10$ –15 per group). Error bar, SEM.

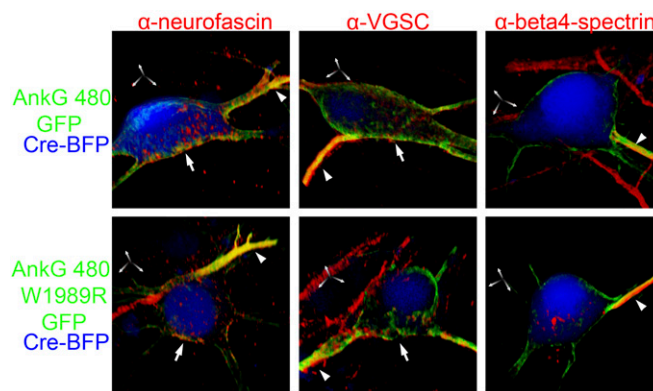


Fig. 58. W1989R 480-kDa ankyrin-G fully restores AIS proteins on the somatodendritic membrane and the functional AIS of ankyrin-G KO neurons. W1989R 480-kDa ankyrin-G accumulates VGSC, neurofascin, and beta-4 spectrin on the AIS as well as VGSC and neurofascin on the somatodendritic membrane. Arrow heads denote proteins concentrated on the AIS as marked by ankyrin-G. Arrows indicate clusters on the somatodendritic membrane colocalized with ankyrin-G. (Scale bar: 5 μm in all axes.)

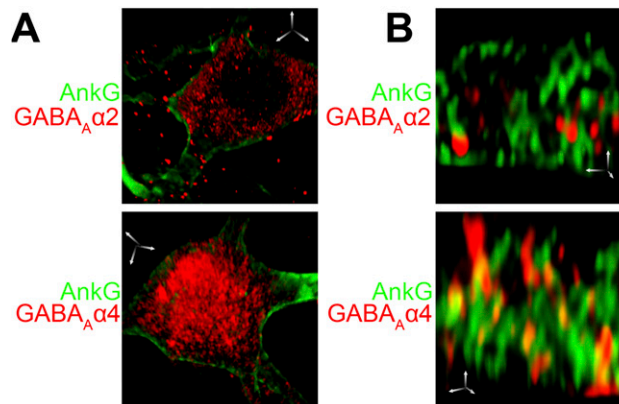


Fig. 59. Ankyrin-G colocalizes with extrasynaptic receptor subunit α4 but not synaptic subunit α2. (A) In WT neurons, both GABA_A receptor subunits α2 and α4 appear punctate on the somatodendritic membrane. (Scale bar: 5 μm in all axes.) (Scale bar: 5 μm in all axes.) (B) Ankyrin-G colocalizes with extrasynaptic receptor α4 subunit in somatodendritic microdomains but is excluded from sites of synaptic receptor α2 subunit. (Scale bar: 1 μm in all axes.)

